Journal of Translational Medicine

RESEARCH

Open Access

DB-1314, a novel DLL3-targeting ADC with DNA topoisomerase I inhibitor, exhibits promising safety profile and therapeutic efficacy in preclinical small cell lung cancer models

Shengchao Lin[1*], Yu Zhang[1], Jun Yao[1], Junjie Yang[1], Yang Qiu[1], Zhongyuan Zhu[1] and Haiqing Hua[1*]

Abstract

Background Delta-like ligand 3 (DLL3) is highly expressed on the cell surface of small cell lung cancer (SCLC), one of the most lethal malignancies, but minimally or not in normal tissues, making it an attractive target for SCLC. However, none of the DLL3-targeting antibody-drug conjugates (ADCs) have been approved for SCLC therapy yet. We developed DB-1314, the new anti-DLL3 ADC composed of a novel humanized anti-DLL3 monoclonal antibody (DB131401) conjugated with eight molecules of P1021 (topoisomerase I inhibitor), and described its preclinical profiles.

Methods The binding epitope for DB131401 and Rovalpituzumab was tested by biolayer interferometry. The binding affinity and specificity of DB-1314 to DLL3 and other homologous proteins were respectively measured by surface plasmon resonance and enzyme-linked immunosorbent assay. Internalization, bystander effects, and antibody-dependent cell-mediated cytotoxicity (ADCC) were assessed by respective assay. DLL3 was quantified by antibodies bound per cell assay and immunohistochemistry. In vitro and *in vivo* growth inhibition studies were evaluated in SCLC cell lines, and cell line/patient-derived xenograft models. The safety profile was measured in cynomolgus monkeys.

Results DB-1314 induces potent, durable, and dose-dependent antitumor effects in cells in vitro and in cell/patient-derived xenograft models in vivo. The killing activity of DB-1314 mechanically arises from P1021-induced DNA damage, whereby P1021 is delivered and released within tumor cells through DLL3-specific binding and efficient internalization. Bystander effects and ADCC also contribute to the antitumor activity of DB-1314. DB-1314 displays favorable pharmacokinetic and toxicokinetic profiles in rats and cynomolgus monkeys; besides, DB-1314 is well-tolerated at a dose of up to 60 mg/kg in monkeys.

*Correspondence:
Shengchao Lin
shengchao.lin@dualitybiologics.com
Haiqing Hua
haiqing.hua@dualitybiologics.com

Full list of author information is available at the end of the article

Conclusions These results suggest that DB-1314 may be a candidate ADC targeting DLL3 for the treatment of DLL3-positive SCLC, supporting further evaluation in the clinical setting.

Keywords DLL3, Antibody-drug conjugate, Small cell lung cancer (SCLC) therapy, Preclinical

Background

Small cell lung cancer (SCLC) is a most aggressive lung neuroendocrine tumor with a propensity to early metastasis, accounting for approximately 15% of all lung cancers [1]. SCLC patients commonly developed disease relapse and resistance following transient initial response to first-line standard-of-care (SoC) platinum-based chemotherapy with or without radiotherapy, leading to a poor 5-year overall survival (OS) of below 7% [2, 3]. Despite about 2–3 month OS improvement with the introduction of immune checkpoint inhibitors in the first-line setting, CASPIAN and IMpower133 trials demonstrated that most SCLC patients progressed while on maintenance immunotherapy [4, 5]. The downregulation of major histocompatibility complex molecules, failure of antigen presentation, and high intratumoral heterogeneity may contribute to the resistance to immunotherapy in SCLC [6–9]. Targeting an alternative cancer cell surface protein presents a promising strategy, potentially improving the prognosis of SCLC patients.

Delta-like ligand 3 (DLL3), an inhibitory ligand of the NOTCH pathway, is recognized as a key role in neuroendocrine differentiation and SCLC tumorigenesis driver [10, 11]. Despite low cytoplasmic expression in normal tissues, DLL3 is highly expressed in approximately 85% of SCLC cells and trafficked to the cell surface [12, 13]. Overexpressing DLL3 has been preclinically implicated in promoting SCLC growth, migration, and invasion and developing resistance to chemotherapy, thus diminishing survival outcomes [14, 15]. The differential expression profiles between normal and tumor tissues and function characteristics underscore DLL3 an appealing, tumor-selective therapeutic target. Several approaches targeting DLL3, such as Chimeric Antigen Receptor (CAR)-T-cell therapies (i.e. AMG 119) and bispecific T-cell engager (BiTE; i.e. tarlatamab), have shown therapeutic benefits (objective response rate [ORR], 25-40%; progression-free survival [PFS], 3.7–4.9 months) in SCLC [16–19]. Notwithstanding, there is a caveat of secondary T-cell lymphomas for CAR-T-cell therapies and cytokine release syndrome/immune effector cell-associated neurotoxicity syndrome for BiTE [18, 20–22]. Overall, there remains an urgent need for anti-DLL3 therapeutic agents with different mechanisms of action for SCLC patients.

Antibody-drug conjugates (ADCs) could deliver cytotoxic payload inside tumor cells through the specific binding to the cell surface and efficient internalization, thereby reducing the off-target systemic toxicity and enhancing therapeutic index (TI) [23]. Additionally, given that ADCs could induce immunogenic cell death and thus enhance antitumor immune responses, ADCs could also potentially serve as a therapeutic companion for strategically combining with classical immunotherapies [24, 25]. Rovalpituzumab tesirine (Rova-T), a first-in-class DLL3-targeted ADC for SCLC, has demonstrated early efficacy signs in the later-line settings; however, toxicity related to payload pyrrolobenzodiazepine (PBD; DNA cross-linking agent) limited the dosage required to achieve maximal efficacy [26, 27]. Considering dose-limiting toxicity independent of DLL3 and the unique pattern of DLL3 in SCLC, anti-DLL3 ADC remains a promising therapeutic approach for SCLC [12, 13, 27].

DB-1314 is a novel anti-DLL3 ADC, comprising DB131401 (a fully humanized anti-DLL3 hIgG1 antibody), conjugated with P1021 (topoisomerase I inhibitor [TOPIi]) via a peptidyl linker. As conjugated in approved Fam-trastuzumab deruxtecan-nxki (ENHERTU), payload deruxtecan (DXd) functions through topoisomerase inhibition and achieves a high drug antibody ratio (DAR) [23, 28]. We thus reasoned that the utilization of cytotoxic warhead P1021, differing in mechanism from PBD, may enable DB-1314 to succeed where Rova-T did not. Here, this study described the preclinical profiles of DB-1314 and demonstrated the mechanism for the potent antitumor activity of DB-1314.

B7H3 is also overexpressed in SCLC tumor tissues but rarely observed in normal tissues, becoming an attractiv target for ADC development [29]. DS-7300 is a ADC targeting B7H3, conjugated with Dxd payload, and has preliminarily demonstrated objective response rate of about 52% and duration of response of 5.9 months in patients with previously treated SCLC [30]. As such, we also focus on the comparison of preclinical activity of DB-1314 with B7H3-targeting ADC DS-7300.

Methods

Antibodies and ADCs

Rovalpituzumab was produced with the published amino acid sequence. DB-1314 was composed of DB131401, a maleimide glycyn-glycyn-phenylalanyn-glycyn (GGFG) peptide linker, and P1021 with the DAR value of 8. Rovalpituzumab-P1021 or isotype (iso)-ADC was composed of Rovalpituzumab or isotype control IgG1 (iso-IgG1), GGFG linker, and P1021 with DAR of 8. DS-7300 (ifinatamab deruxtecan) was synthesized according to the published amino acid sequence and DXd structure. The four inter-strand disulfide bonds of antibodies were reduced to eight cysteine residues by tris(2-carboxyethyl)

phosphine. The linker and payload were connected as described previously [31]. Linker-payload was conjugated to the cysteine residues using a conventional strategy [32].

Hydrophobic interaction chromatography (HIC) for DAR measurement

DAR was measured using a butyl HIC column (TSK-gel Butyl-NPR 4.6×35 mm 2.5 μm; Tosoh Bioscience, Japan) on an Agilent 1260 Infinity II HPLC system equipped with ultraviolet detection at 280 nm. Mobile phase A consisted of 1.5 M $(NH_4)_2SO_4$ and 50 mmol/L K_2HPO_4 at pH 7.0, while mobile phase B contained 21.3 mmol/L KH_2PO_4, 28.6 mmol/L K_2HPO_4, and 25% (v/v) isopropanol at pH 7.0. The gradient program was as follows: B %: 0-25% (0–1 min, flow rate 0.8 mL/min), 25% (1–3 min, flow rate 0.6 mL/min), 25-80% (3–13 min, flow rate 0.6 mL/min), 80% (13–17 min, flow rate 0.6 mL/min), 80%-0% (17–17.1 min, flow rate 0.5 mL/min), 0% (17.1–25 min, flow rate 0.7 mL/min).

Cell lines

Tumor cell lines, including SHP-77 (ATCC, Cat# CRL-2195), DMS53 (ATCC, Cat# CRL-2062), NCI-H82 (ATCC, Cat# HTB-175) and Raji (ATCC, Cat# CCL-86) were purchased from the ATCC and cultured in the corresponding media (SHP-77, NCI-H82 and Raji cells in RPMI-1640 medium [Gibco, USA]; DMS53 in Waymouth's MB 752/1 medium [Sigma, USA] with a 10% fetal bovine serum (FBS; Hyclone, USA) at 37 °C in a 5% CO_2. HEK293-DLL3 (Genomeditech, Cat# GM-C12896) was purchased from Genomeditech (Shanghai, China) and cultured in the DMEM medium [Gibco, USA] with a 10% FBS. All cell lines tested negative for mycoplasma contamination.

Immunohistochemistry (IHC)

IHC staining for DLL3 and B7H3 was performed using the rabbit antibody clone (Cell Signaling, USA; Cat#71804 for DLL3 and Cat#14058 for B7H3) on formalin-fixed, paraffin-embedded sections from patient-derived xenograft (PDX) models and 33 human cancer tissue microarrays (TMAs) (Wanke, China). All samples were processed on the BOND RX Fully Automated Research Stainer (Leica Microsystems, USA) as per the manufacturer's instructions. All images were acquired using NanoZoomer-HT 2.0 Image system (Hamamatsu, Japan) at 40 times magnification (40×). The expression intensities of membranous DLL3 and B7H3 were presented with a histochemical scoring system (H-score) as follows: 0 (H-score 0–9; negative), 1+ (H-score 10–99; weak), 2+ (H-score 100–199; moderate), and 3+ (H-score 200–300; strong).

Biolayer interferometry (BLI) for epitope binning

Two antibodies were detected for competitiveness with each other based on the Gator BLI system (ProbeLife, China). Epitope binning was performed in a tandem setup with His-tagged human DLL3 (60 nM) immobilized on biosensors. Rovalpituzumab at a saturating concentration of 100 nM was applied for 300 s, followed by either Rovalpituzumab or DB131401 at the same concentration and time. The increment of layer thickness in the last step was an indicator of non-overlapping epitopes. The running buffer was a mixture of 10 mM phosphate-buffered saline (PBS; pH 7.4), 0.02% Tween 20, and 0.2% bovine serum albumin.

Surface plasmon resonance (SPR) for binding affinity

The binding affinity of DB131401 to human DLL3 was assessed using Biacore T200 (Cytiva, USA) as per the manufacturer's protocol. Briefly, DB131401 was diluted to 60 nM and immobilized on Series S Protein A Sensor Chip (Cat# 29127556; Cytiva, USA), followed by loading a two-fold serial dilution (starting at 300 nM) of recombinant human His-tagged DLL3 protein (Sanyoubio, China) in HBS-EP+buffer (Cytiva, USA) at a flow rate of 30 μL/min with 180 s of association and 300 s of dissociation. Washing was required to remove excess proteins from biosensors before immersing different sets of antibodies. The association of antibodies was monitored on the sensorgram for epitope binning. Data for binding affinity, including the association rate (Ka), the dissociation rate (Kd), and the dissociation equilibrium constant (KD) values were calculated using the BIAevaluation software (Cytiva, USA) by fitting the global analysis of the association/dissociation curves to bivalent binding model.

Enzyme-linked immunosorbent assay (ELISA) for binding specificity

The immunoplates were respectively coated 2 μg/mL human DLL1 (ACRO, Cat# DL1-H52H8) or human DLL4 (ACRO, Cat# DL4-H5227) or Cynomolgus DLL3 (ACRO, Cat# DL3-C52H3) recombinant proteins overnight at 4 °C, washed, blocked with 5% PBSM at room temperature for 2 h, and then incubated with serial dilutions of DB131401, Rovalpituzumab, or human IgG1 isotype control for an hour. After washing, goat anti-human IgG Fc-horseradish peroxidase (1:4000; Sigma-Millipore, USA) was added to the plate for another hour followed by the visualization with 3,3',5,5'-tetramethylbenzidine substrate. The absorbance at 450 nm was measured using a microplate reader (SpectraMax Mini; Molecular Devices, China).

Internalization assay

HEK293 cells stably and highly expressing human HER3 (H_DLL3 HEK293) were established by lentivirus transduction encoding human DLL3 (genomeditech, Cat# GM-C12896). Following the resuspension in the corresponding complete medium, SHP-77 and H_DLL3 HEK293 cells were seeded at 1×10^4 cells/well in a 96-well plate and then incubated overnight at 37 °C under 5% CO_2. Antibodies including DB131401, Rovalpituzumab, and human IgG1 isotype control were labeled with Incucyte® Human Fabfluor-pH Red Antibody Labeling Reagent (Sartorius, Germany) at 1:3 molar ratio for 15 min and subsequently added to cells. Imaging was captured at the indicated time points by the Incucyte® Live-Cell Analysis System (Sartorius, Germany) and internalization intensity was assessed using the IncuCyte® software (Sartorius, Germany).

Bystander killing effect assay

Firefly luciferase-transfected Raji (Raji-Luc) cells (2000 cells/well) were seeded alone or mixed with an equal number of DLL3-positive NCI-H82 cells into a 96-well plate, followed by treatment with DB-1314 or iso-P1021. After 5-day incubation, the viability of Raji-Luc cells was measured with SteadyGlo® Luciferase Assay System (Promega) according to the manufacturer's instructions. Bystander activity elicited by DLL3-targeting ADC was demonstrated by the reduced viability of Raji-Luc cells.

Antibody-dependent cell-mediated cytotoxicity (ADCC)

ADCC was evaluated using the lactate dehydrogenase (LDH) Cytotoxicity Assay Kit (Beyotime; China). Briefly, human peripheral blood mononuclear cells (PBMCs, effector cells; 4×10^6 cells/mL) and NCI-H82 (target cells; 2×10^5 cells/mL) cells were mixed at an effector-to-target (E: T) ratio of 5:1 and incubated with 1 or 10 nM DB-1314 or iso-P1021 at 37 °C for approximately 4 h. Then, LDH release was detected 30 min after target cell lysis and quantified by measuring the absorbance at 490 nm using the microplate reader (SpectraMax Mini; Molecular Devices, China). Cytotoxicity was calculated using the following formulas: % cytotoxicity = (optical density $[OD]_{\text{experimental release}} - OD_{\text{spontaneous effector cell release + spontaneous target cell release}}$)/($OD_{\text{maximum release}} - OD_{\text{spontaneous release}}$) × 100%.

In vitro cell viability assay

Cells were seeded into 96-well plates at 3000 cells/well for NCI-H82, 6000 cells/well for SHP-77, 5000 cells/well for DMS53, and 2000 cells/well for LU2514 PDC (patient-derived cell, provided by CrownBio). After overnight incubation, a serially diluted solution of ADCs was added. Cell viability was evaluated after 5 days using the CellTiter-Glo® Luminescent Cell Viability kit (Promega; USA) according to the manufacturer's instructions. Luminescence was measured by EnVison Multi-Mode Microplate Reader (PerkinElmer, USA). Concentration-response curves and half-maximal inhibitory concentration (IC_{50}) values were generated by nonlinear regression using a sigmoidal curve fit with variable slope in Graph Pad Prism. Assays were performed in triplicate for each data point. GraphPad Prism software was used for curve fitting. Differences between the two groups were analyzed by a standard Student t-test. $P<0.05$ was considered statistically significant.

DLL3 quantification by antibodies bound per cell (ABC) assay

The assay aimed to evaluate the expression level of DLL3 on selected cell lines. In principle, DLL3 density in cells was measured by the relative number of anti-human DLL3 antibodies bound on each cell surface. ABC was measured using the Quantibrite™ PE Quantitation Kit (BD Biosciences; Cat# 340495). The protocol was followed according to the manufacturer's instructions (https://www.bdbiosciences.com/content/bdb/paths/generate-tds-document.us.340495.pdf). Briefly, excess PE-conjugated anti-human DLL3 antibodies (Biotechne Cat# FAB4315P) were mixed and bound to the cells and analyzed on flow cytometry (BD Accuri C6). Median fluorescence intensity was measured and translated into the number of ABC calibrated with BD Quantibrite™ PE beads.

In vivo efficiency studies

All animal studies were approved by the Institutional Animal Care and Use Committee guidelines of Gempharmatech Co., Ltd. (China) or Crownbio Co., Ltd. (China).

Cell line-derived xenograft (CDX) study

Female NCG or BALA/c-nude mice (18–25 g body weight, provided by GemPharmatech Co. Ltd.) were implanted subcutaneously in the right upper flank region with approximately 5-7.5×10^6 DMS53, SHP-77, or NCI-H82 tumor cells. When the average tumor volumes reached about 100–150 mm^3, mice were randomized by tumor sizes into treatment and control groups (5 mice/group) and then intravenously given vehicle control (PBS), non-binding control ADC (isotype-P1021), DB-1314, or Rovalpituzumab-P1021 at the stated doses (day 0).

PDX study

LU2514, LU5188, LU5215, and LU5266 PDX models were acquired from HuPrime® (CrownBio; USA). Tumor fragments (diameter, 2–3 mm) harvested from these models were subcutaneously implanted in female NOD/SCID or BALA/c-nude mice (20–25 g body weight, provided

by Crownbio Co., Ltd.). Once the tumor grew to the desired volumes of approximately 140–160 mm^3, mice were grouped as described above and intravenously or intraperitoneally injected with vehicle control, DB-1314, or Rovalpituzumab-P1021, DS-7300, or topotecan (MedChemExpress, Cat# HY-13768 A) as indicated (day 0).

Specific pathogen-free mice (6–8 weeks old) were housed in the pathogen-free conditions. Body weight and tumor size were measured twice weekly and tumor volumes were calculated with (length × $width^2$)/2. The antitumor activity was evaluated by tumor growth inhibition (TGI, %). TGI% was calculated as TGI% = [1-(T_i-T_0)/(C_i-C_0)] x100%, where C_0 and T_0 are the mean tumor volume of vehicle and treatment groups at study start, C_i and T_i stand for the mean tumor volume of vehicle and treatment groups on a given day. Statistical analyses were performed using two-way ANOVA for multigroup comparisons. A P-value≤0.05 was considered statistically significant. Animals were euthanized if they displayed weight loss>20%, tumor volume exceeding 3 cm^3, or indicated adverse symptoms.

Toxicokinetics in cynomolgus monkeys

Cynomolgus monkeys (age, 3.5-4 years; weight, 2.7–4.9 kg) were obtained from SuZhou XiShan Laboratory Animal Co., Ltd. (China) and used for repeated-dose toxicokinetic study. Two monkeys per sex per group were intravenously administered with 60 mg/kg DB-1314 at 3-week intervals for two doses. Clinical signs, general conditions, body weight, food consumption, electrocardiography examinations, and clinical pathology parameters were monitored at indicated time points throughout the study. Monkeys were sacrificed on day 7 following the second administration for gross necropsy and histopathologic examinations. Blood samples for toxicokinetics were obtained from each group before the first dosing and at 0, 0.667, 2.5, 6.5, 24.5, 48.5, 72.5, 120.5, 168.5, 336.5, and 504.5 h after administration. The concentrations of total antibody and ADC (DB-1314) in serum were determined by ELISA, while the small molecule (P1021) was quantified by liquid chromatography-mass spectrometry/mass spectrometry. Concentration-time profiles were performed to determine the toxicokinetic parameters using a non-compartmental method in the Phoenix software version 6.3 (Pharsight, USA).

Results

DLL3 is a promising ADC molecule target in SCLC

To characterize the expression patterns of DLL3 on SCLC, IHC staining for DLL3 was conducted on TMA from SCLC patients. Given that DS-7300, a novel B7H3-directed DXd ADC, demonstrated a manageable safety profile and robust and durable efficacy in patients with heavily pretreated SCLC [12, 33], we also detected the expression patterns of B7H3 on SCLC TMA. Among 33 SCLC tumors, 27 (81.8%) samples showed staining positive for DLL3 and 30 (90.9%) demonstrated B7H3 expression (Fig. 1A and Supplementary Figure S1). Besides, the

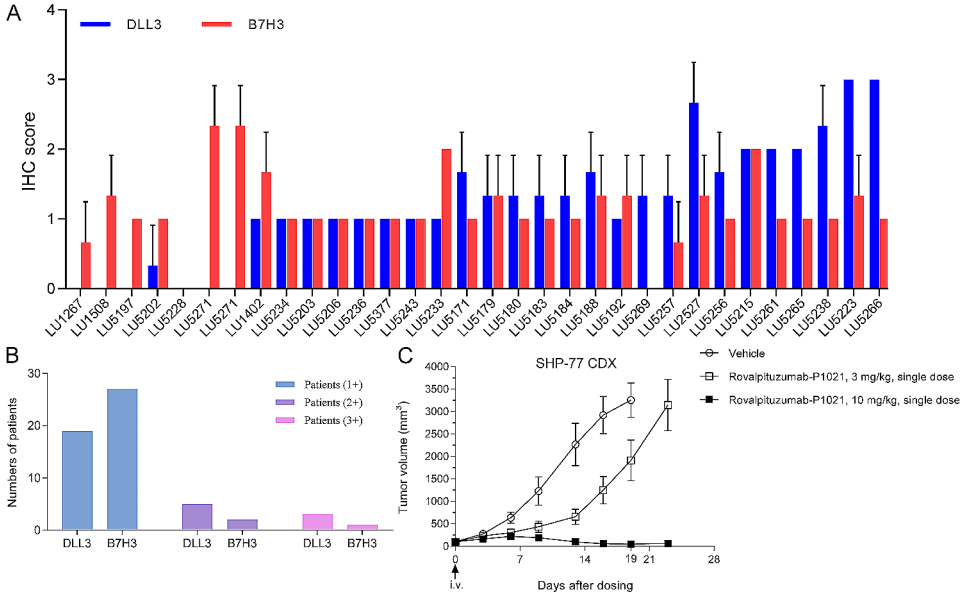

Fig. 1 DLL3 is a promising target for ADC development in SCLC. **(A-B)** DLL3 and B7H3 expressions in a tissue microarray of 33 human SCLC samples were measured by immunohistochemistry. Staining intensity: 1+, weak; 2+, moderate; 3+, strong. Data were representative of three different experiments and expressed as the mean ± SEM. **(C)** Tumor volume was measured twice weekly after dosing with anti-DLL3 ADC (proof of concept) Rovalpituzumab-P1021 or vehicle control in the female BALB/c-Nude mice bearing SHP-77 cancer cells

Abbreviations: IHC, immunohistochemistry; i.v., intravenous injection; ADC, antibody-drug conjugate; SCLC, small cell lung cancer; DLL3, Delta-like ligand 3; CDX, Cell line-derived xenograft; SEM, standard error of the mean

similar staining pattern of DLL3 and B7H3 (weak staining 1+, 70.4% vs. 90%; moderate staining 2+, 18.5% vs. 6.7%; strong staining 3+, 11.1% vs. 3.3%) in these DLL3/B7H3-positive tumors (Fig. 1B) suggested the low/medium prevalence of these two proteins in SCLC. Our comparative expression profile of the DLL3 and B7H3 supported the development of DLL3 as a target for a therapeutic ADC. Furthermore, while DLL3 and B7H3 overlapped with respect to tissue localization, they also showed exclusivity, suggesting the opportunity for DLL3-ADC in patients insensitive to B7H3-ADC.

Then, we generated a DLL3-ADC Rovalpituzumab-P1021 (DAR, 8) for the proof of concept. This ADC comprised humanized IgG1 mAb Rovalpituzumab (Heavy Chain S220C back mutation) linked to P1021 (TOPIi of DualityBio's proprietary) via a maleimide tetrapeptide-based cleavable linker. Given that PBD-related toxicities led to the clinical failure of Rova-T, we replaced PBD with TOPIi with different mechanisms as the potential payload for this proof-of-concept ADC. The DLL3-positive SHP-77 CDX model was used to evaluate the antitumor activity in vivo of single-dose Rovalpituzumab-P1021 and the tested animals showed complete tumor regression (Fig. 1C). Together, these results further validated the feasibility of DLL3-TOPIi ADC in SCLC.

Generation and characterization of DLL3-TOPIi ADC DB-1314

The aforementioned findings prompted the development of DB-1314, a new targeting-DLL3 therapeutic ADC. It was engineered by conjugating anti-DLL3 IgG1 monoclonal antibody (mAb) DB131401 to TOPIi P1021 via a peptidyl linker. HIC showed a homogeneous drug distribution, with a DAR of approximately eight (Fig. 2A). DB131401 is a fully humanized mAb with a binding epitope differentiating from Rovalpituzumab. Epitope binning by BLI detection revealed that DB131401 did not compete with Rovalpituzumab for a similar epitope (Fig. 2B). The binding affinity (KD) of DB131401 for human DLL3 was 2.17 nM as assessed by SPR (Fig. 2C). Similarly to Rovalpituzumab, DB131401 did not bind rodent DLL3 (data not shown). Furthermore, the results from ELISA demonstrated no cross-reactivity with DLL1 or DLL4 (Supplementary Figures S2A and S2B), suggesting the binding specificity of DB131401 for DLL3. As intracellular delivery of cytotoxic agents is the rationale for ADC activity, [23] we first confirmed the internalization of DB-1314 into DLL3-positive SCLC cells. Internalization kinetics of DB131401 and Rovalpituzumab tagged with Incucyte® Fabfluor-pH sensitive dye was assessed in SHP-77 cells and human DLL3 high expressing HEK293 (H_DLL3 HEK293) cells using Incucyte. Compared with the isotype IgG1 control, DB131401 and

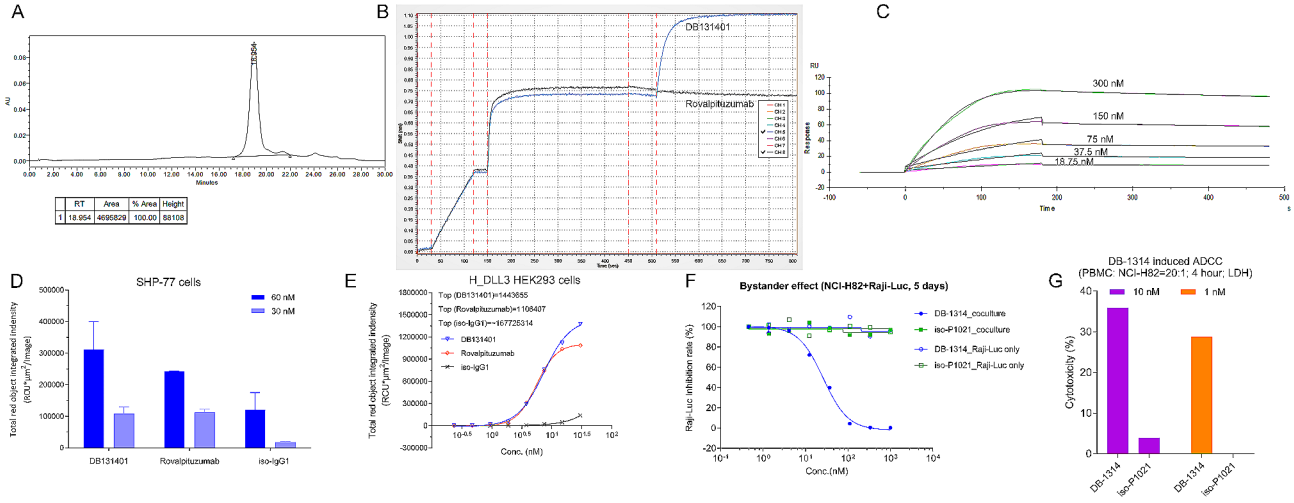

Fig. 2 In vitro property characterization of anti-DLL3 ADC DB-1314. **(A)** Conjugated drug distribution was measured by hydrophobic interaction chromatography. **(B)** Epitope binning of DB131401 and Rovalpituzumab by BLI. His-tagged human DLL3 (60 nM) was loaded onto biosensor, followed by binding of the first antibody Rovalpituzumab at saturating concentration of 100 nM. Subsequently, either the saturation antibody Rovalpituzumab or the completion antibody DB131401 was applied. CH5 represented 100 nM DB131401. CH8 represented 100 nM Rovalpituzumab. Increment of layer thickness in the last step suggested that the epitopes of the two antibodies did not overlap. **(C)** Affinity of DB131401 and Rovalpituzumab binding to human DLL3 was characterized using SPR. Internalization of DB131401 and Rovalpituzumab tagged with Incucyte® Fabfluor-pH sensitive dye in SHP-77 cancer cells **(D)** and highly expressing human HER3 HEK293 (H_DLL3 HEK293) cells **(E)** was analyzed by Incucyte® Live-Cell Analysis System and quantified using the IncuCyte® software. **(F)**In vitro bystander killing effect of DB-1314. DLL3-positove NCI-H82 cells and DLL3-negative Raji-Luc cells were cocultured for 5 days and incubated with DB-1314, followed by the measurement of viable Raji-Luc cell numbers by detecting the luciferase activity using the luminometer. **(G)** ADCC activity of DB-1314 was measured using isolated PBMCs cocultured with NCI-H82 cells

Abbreviations: BLI, biolayer interferometry; PBMC, peripheral blood mononuclear cell; ADCC, antibody-dependent cell-mediated cytotoxicity; LDH, lactate dehydrogenase; ADC, antibody-drug conjugate; DLL3, Delta-like ligand 3; SPR, surface plasmon resonance; iso-IgG1, isotype IgG1; conc., concentration

Rovalpituzumab were efficiently internalized into cells, with a higher internalization rate of DB131401 (Fig. 2D and E). Bystander killing is important in tumors with heterogeneous target expression [34]. To test the bystander activity of DB-1314, co-cultures of DLL3-positive NCI-H82 and DLL3-negative Raji-luciferase (Raji-Luc) cells were treated with DB-1314; and the viability of Raji-luc cells was assessed by measuring the luciferase activity using the luminometer. As expected, DB-1314 elicited bystander activity, as demonstrated by the reduction of Raji-Luc cells (Fig. 2F). The lack of direct activity of DB-1314 on DLL3-negative Raji-luc cells was confirmed by treatment in the absence of NCI-H82 cells (Fig. 2F). These data validated that the cell permeability of P1021 enabled DB-1314 to induce bystander activity. ADCC is one of the mechanisms of tumor cell killing for therapeutic antibodies with wild-type Fc [35]. DB131401 mediated ADCC in NCI-H82 cells in the presence of PBMC (Fig. 2G).

Taken together, these results demonstrated that DB-1314 exerted a high affinity and specificity to DLL3, high internalization, and could induce bystander killing effects and ADCC, potentially representing a new promising anti-DLL3 ADC therapy for SCLC following the failure of Rova-T.

DB-1314 exhibits potent cytotoxic activity in vitro

We then investigated the effect of DB-1314 on the proliferation inhibition of DLL3-positive cancer cells in vitro, and compared it with Rovalpituzumab-P1021. DLL3 expression levels on the membrane of the DMS53, NCI-N82, and SHP-77 cell lines and LU2514 PDC were assessed using QuantiBRITE™ PE beads by flow cytometry. The ABC of DMS53 (Fig. 3A), NCI-N82 (Fig. 3B), and SHP-77 (Fig. 3C) cells were respectively 323, 608, and 444, indicating the positive but low expression of DLL3 on the cell surface; whereas the ABC was 2967.64 for LU2514 (Fig. 3D). Of note, DB-1314 exhibited potent growth-suppressive activity against all tested DLL3-positive cells, independent of the specific DLL3 expression magnitude; the IC_{50} values for DMS53, NCI-N82, and SHP-77cell lines and LU2514 PDC were calculated as 45, 37, 538, and 147.82 nM, respectively (Fig. 3A and D). Besides, there was a comparable inhibitory effect of Rovalpituzumab-P1021 on these tested cells to that of DB-1314 (Fig. 3A and D). Together, these results suggested the remarkable cytotoxic killing of DB-1314 against DLL3-positive SCLC cells, even those with low surface DLL3 expressions (<1000 molecules per cell was defined as low expression of DLL3 [36]).

DB-1314 exhibits significant antitumor effects in vivo

We further examined the antitumor activity in CDX models with low DLL3 expression. Tumor-bearing mice

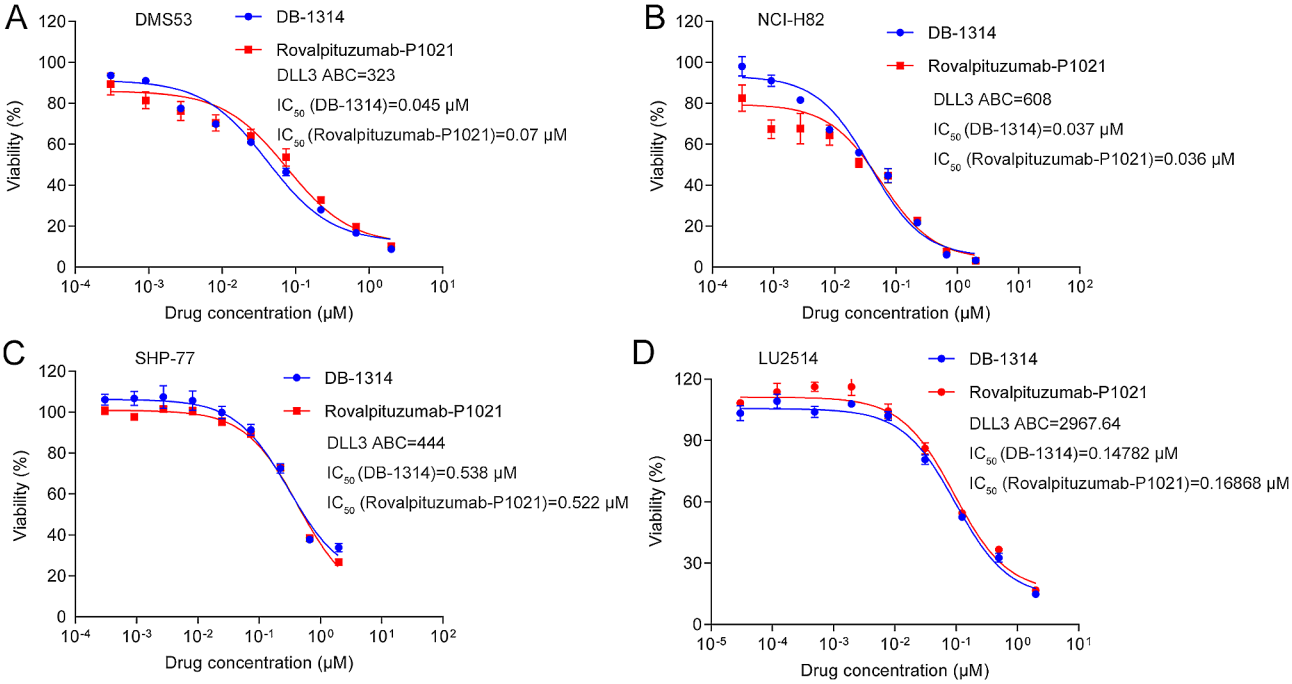

Fig. 3 In vitro cytotoxicity of DB-1314. In vitro cytotoxicity of DB-1314 and Rovalpituzumab-P1021 was measured 6 days after treatment in **(A)** DMS53, **(B)** NCI-H82, **(C)** SHP-77cancer cell lines, and **(D)** LU2514 patient-derived cells. Data were representative of three different experiments and expressed as the mean ± SEM

Abbreviations: ABC, antibodies bound per cell; DLL3, Delta-like ligand 3; SEM, standard error of the mean; IC_{50}, half-maximal inhibitory concentration

were intravenously injected with vehicle control, isotype-P1021, Rovalpituzumab-P1021, or DB-1314 at indicated concentrations once a week for one or two doses. Compared with vehicle control and isotype-P1021, DB-1314 and Rovalpituzumab-P1021 exerted significant dose-dependent tumor growth inhibition in mice bearing with NCI-H82 cells (Fig. 4A). In either mice bearing DMS53 cells or mice bearing SHP-77 cells, these two ADCs induced complete tumor regression and sustained antitumor activity over 28 days (Fig. 4B and C).

Generally, PDX models were more clinically relevant because they preserved clinical characteristics, including heterogeneity, molecular diversity, and histological resemblance, of original tumors [37]. We further evaluated the therapeutic effects of DB-1314 in PDX models and additionally focused on the efficacy comparisons with DS-7300, a candidate anti-B7H3 ADC against SCLC [33]. IHC showed positive but heterogeneous expression of DLL3 and B7H3 in SCLC PDX models (Fig. 5). Regardless of the relative expression level of DLL3 and B7H3, DB-1314 exhibited comparable or superior antitumor response than DS-7300 administered at the same doses in LU2514 (H score, 153.68 vs. 96.26; both complete tumor regression; Fig. 5A), LU5188 (H score, 179.78 vs. 102.23; complete tumor regression vs. tumor regrowth; Fig. 5B), LU5215 (H score, 175.11 vs. 240.74; TGI, 83.53% vs. 106.96%; Fig. 5C), and LU5266 (H score, 267.35 vs. 207.36; TGI, 91.44% vs. 70.01%; Fig. 5D) models. Besides, DB-1314 showed comparable activity with Rovalpituzumab-P1021 in LU5215 (Fig. 5C) and LU5266 (Fig. 5D) PDX. Further, to elucidate the therapeutic advantage of ADC over TopIi-based chemotherapy monotherapy, DB-1314 was compared with topotecan (FDA-approved SoC in second-line SCLC treatment) and demonstrated greater reductions in tumor burden in LU5188 PDX (Fig. 5B). DB-1314 was well-tolerated in tumor-bearing mice, with no obvious body weight loss observed in all PDX models (Fig. 5). Together, DB-1314 could effectively inhibit the growth of SCLC tumors in vivo, suggesting the treatment potential of DB-1314 in the clinical setting.

Safety studies in nonhuman primates

Cynomolgus monkey is an appropriate model for the safety assessment of target-dependent toxicities of DB-1314 because DB131401 mAb binds to cynomolgus monkey DLL3 with similar affinity as humans (Supplementary Fig. 3). Preliminary safety studies investigated DB-1314 every 3 weeks (Q3W×2) at 60 mg/kg dose. After administration of DB-1314 at 60 mg/kg, the animals showed minimal and reversible changes in the hematological system (granulocyte, erythroid) and hepatic function indicators (alanine aminotransferase, aspartate aminotransferase) and slight thymic atrophy (Tables 1 and Supplementary Table 1). With this dosing regimen, the maximum tolerated dose was determined to be greater than 60 mg/kg.

Toxicokinetic profiles of DB-1314 also demonstrated high serum stability in cynomolgus monkeys following intravenous administration at 60 mg/kg (Fig. 6), with similar serum concentration and pharmacokinetic parameters ($T_{1/2}$, 10.58 vs. 9.75 days) of ADC to total Ab throughout the course. A low level of payload P1021 was detected and the serum area under the curve $(AUC)_{0-168.5}$ for total Ab is 72,014 μg*h/mL and for ADC is 72,226 μg*h/mL, suggesting that most Ab remaining in circulation still retained conjugated payload P1021. Together, these data suggested that DB-1314 may achieve high exposure for clinically required therapeutic efficacy in a context of acceptable safety.

Discussion

Compared with conventional cytotoxic chemotherapy, targeted therapy (either small molecule drugs or biological therapeutics) often exhibits improved tumor response and reduced toxicity. SCLC is a highly lethal tumor with a high degree of intratumoral heterogeneity [38]. Despite the identification of various oncogenic drivers (PARP1,

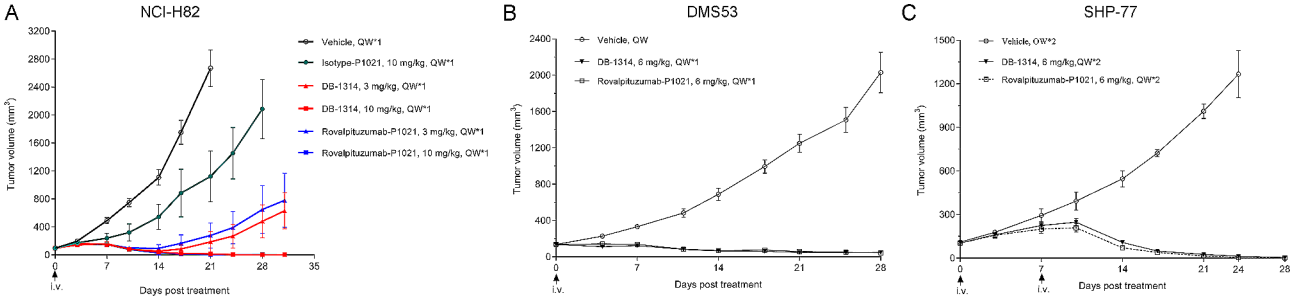

Fig. 4 Antitumor effects in cell-derived xenograft (CDX). Tumor volume was measured twice weekly after treatment with vehicle control, control ADC (isotype-P1021), Rovalpituzumab-P1021, or DB-1314 at indicated doses in 3 CDX models: **(A)** female BALB/c-Nude mice bearing NCI-H82 cancer cells, **(B)** NCG mice bearing DMS53 cancer cells, and **(C)** BALB/c-Nude mice bearing SHP-77 cancer cells. The results were representative of three different experiments and expressed as the mean ± SEM

Abbreviations: SEM, standard error of the mean; ADC, antibody-drug conjugate; QW, once a week; i.v., intravenous injection

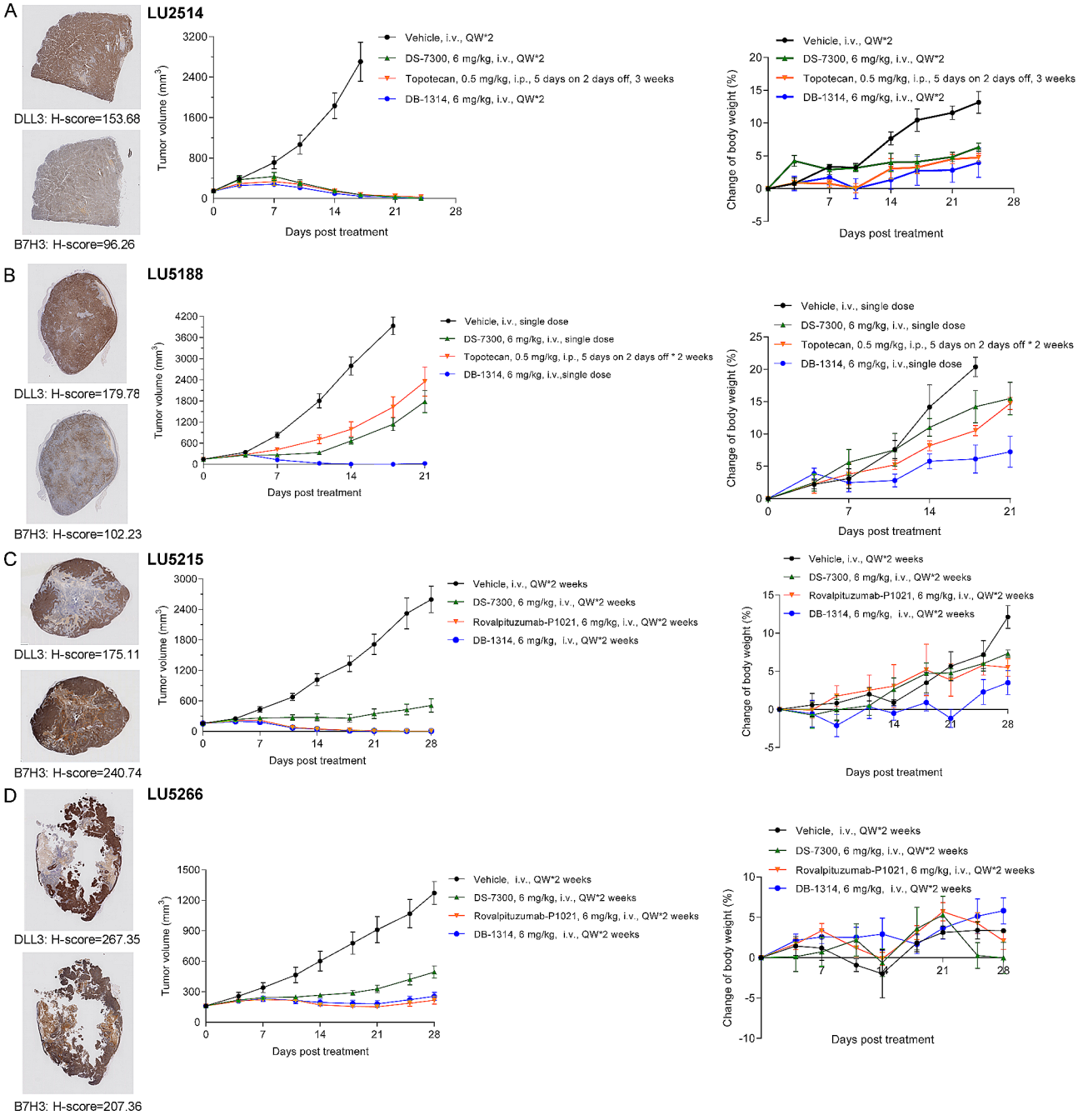

Fig. 5 Antitumor effects in patient-derived xenograft (PDX) models. Representative images and H-scores of DLL3 and B7H3 are shown for each xenograft model. Scale bar, 100 μm. Body weight and tumor volume were measured twice weekly after treatment with vehicle control, Rovalpituzumab-P1021, DB-1314, DS-7300, or topotecan at indicated doses in 4 PDX models: **(A)** female BALB/c-Nude mice bearing LU2514 tumor fragments, **(B)** NOD/SCID mice bearing LU5188 tumor fragments, **(C)** NOD/SCID mice bearing LU5215 tumor fragments, and **(D)** NOD/SCID mice bearing LU5266 tumor fragments. The results were representative of three different experiments and expressed as the mean ± SEM

Abbreviations: DLL3, Delta-like ligand 3; SEM, standard error of the mean; QW, once a week; i.v., intravenous injection; i.p., intraperitoneal injection

CHK1, LSD1, EZH2, etc.) in SCLC over the last few decades, there unfortunately were no survival benefits of targeted therapies for these drivers [39]. DLL3 has recently been identified as an SCLC-specific tumor antigen. Consistently with previously reported wide expression, [12, 13] we also observed the detectable membrane DLL3 expression across 81.8% of SCLC TMAs. However, our IHC staining in PDX models and ABC detection in tumor cell lines, along with previous research, showed low-medium abundance in SCLC [40]. This aligns with concerns raised by Amgen about the potential inadequacy of toxic payloads delivered to cells due to low

Table 1 Safety data in cynomolgus monkeys

Toxicity study of DB-1314 in cynomolgus monkeys	
Dose Regimen	60 mg/kg, Q3W, 2 doses
Clinical observation	Occasional soft feces
Gross necropsy observation	Slight thymic atrophy
Blood biochemistry	Slight decrease in neutrophil Slight increase in AST/ALT

Abbreviations: Q3W, every 3 weeks; AST, aspartate aminotransferase; ALT, alanine aminotransferase

DLL3 expression, and thus Amgen opted to develop BiTE targeting DLL3 and CD3 (tarlatamab) rather than DLL3-directed ADCs. DeLLphi-301 trial has demonstrated ORR of 40% and PFS of 4.9 months in patients with previously treated SCLC at 10 mg tarlatamab every 2 weeks [18].

By contrast, we established an DLL3-directed ADC because the approval of ADC DS-8201 in HER2 low breast cancer demonstrated a promising feasibility for ADC targeting low-expression targets [41]. DS-8201 exemplifies an approach that less toxic DXd rather than MMAE and DM1 as payload enables a higher DAR and sufficient accumulation of therapeutic toxins, improving the TI of ADCs and extending their benefits to tumors with low/negative expressions of target proteins [42, 43]. Given the comparable expression level of DLL3 to B7H3 in our IHC staining, the fact of significant clinical benefits with B7H3-targeting ADC DS-7300 in heavily pretreated SCLC patients also supported the therapeutic potential of DLL3-directed ADC with the DXd payload in SCLC.[37,38] Although Rova-T failed in clinical development due to payload PBD-related narrow therapeutic window, early efficacy signs in the later-line therapy for SCLC were encouraging.[24,25,38] As such, we reason that the replacement of PBD with TopIi could achieve acceptable tolerability and maximize the therapeutic potential of DLL3-targeted ADC in SCLC [28, 42, 44, 45]. Consistent with this hypothesis, Rovalpituzumab-P1021, an ADC comprising a similar antibody to Rova-T conjugated to TOPIi P1021, induced complete tumor regression in CDX models with low DLL3 expression. Together, we further generated DB-1314, a novel fully humanized anti-DLL3 mAb DB131401 conjugated with payload P1021 (DAR 8).

We found significant antiproliferative activity of DB-1314 in several SCLC cell lines even with low surface DLL3 expressions (<1000 molecules per cell) and potent, lasting, and dose-dependent growth-inhibitory effects in CDX models carrying these tumor cells. The process that DB-1314 bound to DLL3 with high affinity and efficiently internalized into tumors followed by the sufficient release of cytotoxic payload may contribute to the antitumor effects observed here. Besides, the high stability of DB-1314 in vivo may reduce degradation of the ADC in plasma and result in therapeutic accumulation of payloads in target tumor cells, ultimately favoring potent P1021-mediated cytotoxicity. Furthermore, similar to the remarkable efficacy of DS-8201 driven by payload TOPIi-mediated bystander killing effect, [42, 46] our investigation has paralleled this mechanism with DB-1314, revealing that P1021 penetrates surrounding cells, resulting in the elimination of the target and neighboring tumor cells. This is particularly advantageous for treating heterogeneous SCLC tumors [34].

Consistent with robust in vitro activity, DB-1314 also demonstrated potent antitumor effects in multiple more clinically relevant PDX models. Of note, although IHC showed a similar staining score of DLL3 to B7H3 in these heterogeneous PDX models, DB-1314 overall exhibited comparable or enhanced inhibitory effects on tumor growth compared to DS-7300. The discrepancies of DAR

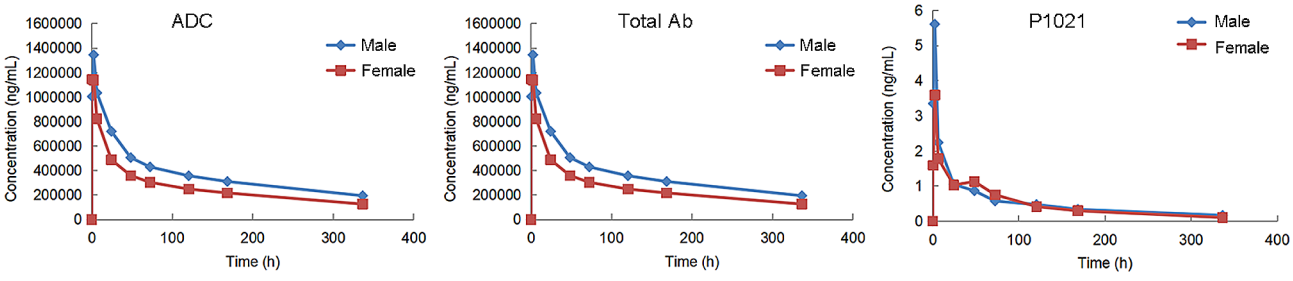

	$AUC_{0\text{-}t}$ (h·μg/mL)			T_{max} (h)			$AUC_{0\text{-}\infty}$ (h·μg/mL)			C_{max} (μg/mL)			$T_{1/2}$ (h)		
	Male	Female	Total	Male	Female	Total	Male	Female	Total	Male	Female	Total	Male	Female	Total
ADC DB-1314	129365	91240	110302	2.5	0.667	1.58	211889	139558	175723	1306	1050	1178	268	240	254
Total Ab	125370	88779	107075	2.5	0.667	1.58	195265	129181	162223	1346	1146	1246	248	220	234
P1021	177	164	171	2.5	2.5	2.5	213	180	197	5.61	3.59	4.60	147	110	128

Fig. 6 Toxicokinetics of DB-1314. Blood samples from cynomolgus monkeys were collected at the indicated time after repeated drug administration for toxicokinetic profile analysis of total antibody, payload P1021, and ADC DB-1314
Abbreviations: ADC, antibody-drug conjugate; Ab, antibody; AUC, area under the curve

(DB-1314, 8 vs. DS-7300, 4 [47]) and payload (DXd vs. P1021) potency in selected PDX models may bias the interpretation of efficacy comparisons. These findings in PDX models may position DB-1314 as a therapeutic alternative in SCLC tumors where DS-7300 shows poor tumor response. Besides, reduced off-target toxicities, including minimal and reversible changes in the hematological system and hepatic function indicators and slight thymic atrophy, were observed at up to 60 mg/kg in monkey study with DB-1314, suggesting the well-tolerance of DB-1314. Together, we reason that DB-1314 may have a wide therapeutic window, enabling SCLC patients to safely achieve a clinically relevant dose and improving the TI.

In addition to its potential as a single agent, DB-1314 may appear as a promising companion for immune-oncology (IO) therapy, synergistically improving the therapeutic benefits. Mechanically, tumor cells undergoing apoptosis following exposure to DB-1314 may emit immune-stimulatory molecules, which promote the recruitment and activation of both the innate and adaptive immune systems [48]. Besides, the Fc region of IgG1 mAbs interacted with the Fc gamma receptor (FcγR) of immune cells, which may elicit ADCC and thus enhance antitumor immune responses [23, 49]. Given the acquired resistance to first-line immunotherapies and the low response rates with pembrolizumab in later-line treatment of SCLC, [50, 51] strategically combined DB-1314 with IO in either first-line or later-line settings should be the focus of future research.

Conclusion

In conclusion, significant preclinical activities may position DB-1314, a newly developed anti-DLL3 ADC, as a promising candidate therapeutic option for heterogeneous DLL3-positive SCLC, deserving further evaluation from bench to bedside.

Abbreviations

DLL3	Delta-like ligand 3
SCLC	Small cell lung cancer
ADCs	Antibody-drug conjugates
ADCC	Antibody-dependent cell-mediated cytotoxicity
SoC	Standard-of-care
OS	Overall survival
CAR	Chimeric Antigen Receptor
TI	Therapeutic index
Rova-T	Rovalpituzumab tesirine
DAR	Drug antibody ratio
PDX	Patient-derived xenograft
TMAs	Tissue microarrays
Ka	Association rate
Kd	Dissociation rate
KD	Dissociation equilibrium constant
LDH	Lactate dehydrogenase
AUC	Area under the curve
IO	Immune-oncology
FcγR	Fc gamma receptor

Supplementary Information

The online version contains supplementary material available at https://doi.org/10.1186/s12967-024-05568-y.

Supplementary figure S1. Representative image of IHC for DLL3 and B7H3 in tissue microarray of 33 human SCLC samplesScale bar, 100 μmAbbreviations: IHC, immunohistochemistry; DLL3, Delta-like ligand 3; SCLC, small cell lung cancer

Supplementary figure S2. Specificity characterization of anti-DLL3 ADC DB-1314Binding specificity of DB131401 to human DLL1 **(A)** and DLL4 **(B)** was analyzed by ELISAAbbreviations: ELISA, enzyme-linked immunosorbent assay; huDLL1, human Delta-like ligand 1; huDLL4, human Delta-like ligand 4; DLL3, Delta-like ligand 3; ADC, antibody-drug conjugate; SEM, standard error of the mean; HRP, horse radish peroxidase; conc., concentration; Abs, antibodies; OD, optical density; ECD, extracellular domain

Supplementary figure S3. Affinity of DB131401 and Rovalpituzumab binding to cynomolgus monkey DLL3 was characterized using ELISAData were representative of at least three different experiments and expressed as the mean ± SEMAbbreviations: ELISA, enzyme-linked immunosorbent assay; CynoDLL3, Cynomolgus Delta-like ligand 3; SEM, standard error of the mean; Abs, antibodies; HRP, horse radish peroxidase; conc., concentration; OD, optical density

Supplementary Material 4

Acknowledgements

Not applicable.

Author contributions

Shengchao Lin and Haiqing Hua designed the research studies and analyzed and interpreted the data. Shengchao Lin and Jun Yao performed the research. Junjie Yang and Yu Zhang provided reagents and performed the druggability stability study. Shengchao and Haiqing Hua wrote the manuscript. Zhongyuan Zhu supervised the study and fund support. All authors read and approved the final manuscript.

Funding

This study was fully supported by Duality Biologics, Ltd.
All authors are employees of Duality Biologics, Ltd., which provided support in the form of salaries for authors and funding for research materials but did not have any additional role in the study design, data collection, and analysis, decision to publish, or preparation of the manuscript.

Data availability

The data that support the findings of this study are available from the corresponding author upon reasonable request.

Declarations

Ethics approval and consent to participate

All animal studies were approved by the Institutional Animal Care and Use Committee guidelines of Gempharmatech Co., Ltd. (China) or Crownbio Co., Ltd. (China).

Consent for publication

Not applicable.

Competing interests

The authors declare that they have no competing interests.

Author details

[1]Department of Research and Development, Duality Biologics, LTD, Unite 1106 868 Yinghua Road, Unite 1106, 201204, Shanghai, P.R. China

Received: 20 June 2024 / Accepted: 3 August 2024
Published online: 14 August 2024

References

1. Cancer.Net. Lung Cancer - Small Cell: Statistics. 2/27. 2023. Accessed 2/27, 2023. https://www.cancer.net/cancer-types/lung-cancer-small-cell/statistics
2. Ganti AKP, Loo BW, Bassetti M, Blakely C, Chiang A, D'Amico TA, et al. Small cell Lung Cancer, Version 2.2022, NCCN Clinical Practice guidelines in Oncology. J Natl Compr Canc Netw. 2021;19:1441–64.
3. Society AC. Lung Cancer Survival Rates|5-Year Survival Rates for Lung Cancer. https://www.cancer.org/cancer/types/lung-cancer/detection-diagnosis-staging/survival-rates.html
4. Goldman JW, Dvorkin M, Chen Y, Reinmuth N, Hotta K, Trukhin D, et al. Durvalumab, with or without tremelimumab, plus platinum-etoposide versus platinum-etoposide alone in first-line treatment of extensive-stage small-cell lung cancer (CASPIAN): updated results from a randomised, controlled, open-label, phase 3 trial. Lancet Oncol. 2021;22:51–65.
5. Liu SV, Reck M, Mansfield AS, Mok T, Scherpereel A, Reinmuth N, et al. Updated overall survival and PD-L1 subgroup analysis of patients with extensive-stage small-cell lung Cancer treated with atezolizumab, carboplatin, and Etoposide (IMpower133). J Clin Oncol. 2021;39:619–30.
6. Gay CM, Stewart CA, Park EM, Diao L, Groves SM, Heeke S et al. Patterns of transcription factor programs and immune pathway activation define four major subtypes of SCLC with distinct therapeutic vulnerabilities. Cancer Cell. 2021;39:346 – 60.e7.
7. Stewart CA, Gay CM, Xi Y, Sivajothi S, Sivakamasundari V, Fujimoto J, et al. Single-cell analyses reveal increased intratumoral heterogeneity after the onset of therapy resistance in small-cell lung cancer. Nat Cancer. 2020;1:423–36.
8. Garassino M, Shrestha Y, Xie M, Lai Z, Spencer S, Dalvi T, et al. MA16. 06 durvalumab ± tremelimumab + platinum-etoposide in 1L ES-SCLC: exploratory analysis of HLA genotype and survival in CASPIAN. J Thorac Oncol. 2021;16:S939.
9. Tian Y, Zhai X, Han A, Zhu H, Yu J. Potential immune escape mechanisms underlying the distinct clinical outcome of immune checkpoint blockades in small cell lung cancer. J Hematol Oncol. 2019;12:67.
10. Augustyn A, Borromeo M, Wang T, Fujimoto J, Shao C, Dospoy PD, et al. ASCL1 is a lineage oncogene providing therapeutic targets for high-grade neuroendocrine lung cancers. Proc Natl Acad Sci U S A. 2014;111:14788–93.
11. Wang XD, Hu R, Ding Q, Savage TK, Huffman KE, Williams N, et al. Subtype-specific secretomic characterization of pulmonary neuroendocrine tumor cells. Nat Commun. 2019;10:3201.
12. Saunders LR, Bankovich AJ, Anderson WC, Aujay MA, Bheddah S, Black K, et al. A DLL3-targeted antibody-drug conjugate eradicates high-grade pulmonary neuroendocrine tumor-initiating cells in vivo. Sci Transl Med. 2015;7:302ra136.
13. Tanaka K, Isse K, Fujihira T, Takenoyama M, Saunders L, Bheddah S, et al. Prevalence of Delta-like protein 3 expression in patients with small cell lung cancer. Lung Cancer. 2018;115:116–20.
14. Furuta M, Kikuchi H, Shoji T, Takashima Y, Kikuchi E, Kikuchi J, et al. DLL3 regulates the migration and invasion of small cell lung cancer by modulating Snail. Cancer Sci. 2019;110:1599–608.
15. Huang J, Cao D, Sha J, Zhu X, Han S. DLL3 is regulated by LIN28B and miR-518d-5p and regulates cell proliferation, migration and chemotherapy response in advanced small cell lung cancer. Biochem Biophys Res Commun. 2019;514:853–60.
16. Byers LA, Chiappori A, Smit M-AD. Phase 1 study of AMG 119, a chimeric antigen receptor (CAR) T cell therapy targeting DLL3, in patients with relapsed/refractory small cell lung cancer (SCLC). American Society of Clinical Oncology; 2019.
17. Paz-Ares L, Champiat S, Lai WV, Izumi H, Govindan R, Boyer M, et al. Tarlatamab, a first-in-class DLL3-Targeted bispecific T-Cell engager, in recurrent small-cell lung Cancer: an Open-Label, phase I study. J Clin Oncol. 2023;41:2893–903.
18. Ahn MJ, Cho BC, Felip E, Korantzis I, Ohashi K, Majem M, et al. Tarlatamab for patients with previously treated small-cell Lung Cancer. N Engl J Med. 2023;389:2063–75.
19. Byers L, Heymach J, Gibbons D, Zhang J, Chiappori A, Rasmussen E, et al. 697 a phase 1 study of AMG 119, a DLL3-targeting, chimeric antigen receptor (CAR) T cell therapy, in relapsed/refractory small cell lung cancer (SCLC). J Immunother Cancer. 2022;10:A728–A.
20. Furlow B. FDA investigates risk of secondary lymphomas after CAR-T immunotherapy. Lancet Oncol. 2024;25:21.
21. Administration USFD. FDA Investigating Serious Risk of T-cell Malignancy Following BCMA-Directed or CD19-Directed Autologous Chimeric Antigen Receptor (CAR) T cell Immunotherapies. https://www.fda.gov/vaccines-blood-biologics/safety-availability-biologics/fda-investigating-serious-risk-t-cell-malignancy-following-bcma-directed-or-cd19-directed-autologous
22. Shimabukuro-Vornhagen A, Gödel P, Subklewe M, Stemmler HJ, Schlößer HA, Schlaak M, et al. Cytokine release syndrome. J Immunother Cancer. 2018;6:56.
23. Fu Z, Li S, Han S, Shi C, Zhang Y. Antibody drug conjugate: the biological missile for targeted cancer therapy. Signal Transduct Target Ther. 2022;7:93.
24. Rudin CM, Reck M, Johnson ML, Blackhall F, Hann CL, Yang JC, et al. Emerging therapies targeting the delta-like ligand 3 (DLL3) in small cell lung cancer. J Hematol Oncol. 2023;16:66.
25. Pascual-Pasto G, McIntyre B, Shraim R, Buongervino SN, Erbe AK, Zhelev DV et al. GPC2 antibody-drug conjugate reprograms the neuroblastoma immune milieu to enhance macrophage-driven therapies. J Immunother Cancer. 2022;10.
26. Rudin CM, Pietanza MC, Bauer TM, Ready N, Morgensztern D, Glisson BS, et al. Rovalpituzumab tesirine, a DLL3-targeted antibody-drug conjugate, in recurrent small-cell lung cancer: a first-in-human, first-in-class, open-label, phase 1 study. Lancet Oncol. 2017;18:42–51.
27. Morgensztern D, Besse B, Greillier L, Santana-Davila R, Ready N, Hann CL, et al. Efficacy and safety of Rovalpituzumab Tesirine in Third-Line and Beyond patients with DLL3-Expressing, Relapsed/Refractory small-cell Lung Cancer: results from the phase II TRINITY study. Clin Cancer Res. 2019;25:6958–66.
28. Siddiqui T, Rani P, Ashraf T, Ellahi A. Enhertu (fam-trastuzumab-deruxtecan-nxki)–Revolutionizing treatment paradigm for HER2-Low breast cancer. Annals Med Surg. 2022;82.
29. Fabrizio FP, Muscarella LA, Rossi A. B7-H3/CD276 and small-cell lung cancer: what's new? Transl Oncol. 2024;39:101801.
30. Johnson M, Awad M, Koyama T, Gutierrez M, Falchook G, Piha-Paul S, et al. OA05. 05 Ifinatamab Deruxtecan (I-DXd; DS-7300) in patients with refractory SCLC: a subgroup analysis of a phase 1/2 study. J Thorac Oncol. 2023;18:S54–5.
31. DUALITY BIOLOGICS (SUZHOU). CO. L. WO2022068878A1-Antitumor compound, and preparation method therefor and use thereof. https://patentscope.wipo.int/search/en/detail.jsf?docId=WO2022068878
32. Lyon RP, Meyer DL, Setter JR, Senter PD. Conjugation of anticancer drugs through endogenous monoclonal antibody cysteine residues. Methods Enzymol. 2012;502:123–38.
33. Paz-Ares L, Johnson M, Girard N, Hann C, Ahn M, Nishio M, et al. 1550TiP phase II, multicenter, randomized, open-label study of DS-7300 in patients (pts) with pre-treated extensive-stage small cell lung cancer (ES-SCLC). Ann Oncol. 2022;33:S1255–6.
34. Staudacher AH, Brown MP. Antibody drug conjugates and bystander killing: is antigen-dependent internalisation required? Br J Cancer. 2017;117:1736–42.
35. Natsume A, Niwa R, Satoh M. Improving effector functions of antibodies for cancer treatment: enhancing ADCC and CDC. Drug Des Devel Ther. 2009;3:7–16.
36. Giffin MJ, Cooke K, Lobenhofer EK, Estrada J, Zhan J, Deegen P, et al. AMG 757, a half-life extended, DLL3-Targeted bispecific T-Cell engager, shows high potency and sensitivity in Preclinical models of Small-Cell Lung Cancer. Clin Cancer Res. 2021;27:1526–37.
37. Hidalgo M, Amant F, Biankin AV, Budinská E, Byrne AT, Caldas C, et al. Patient-derived xenograft models: an emerging platform for translational cancer research. Cancer Discov. 2014;4:998–1013.
38. Patel SR, Das M. Small cell Lung Cancer: emerging targets and strategies for Precision Therapy. Cancers (Basel). 2023;15.
39. Megyesfalvi Z, Gay CM, Popper H, Pirker R, Ostoros G, Heeke S, et al. Clinical insights into small cell lung cancer: Tumor heterogeneity, diagnosis, therapy, and future directions. CA Cancer J Clin. 2023;73:620–52.
40. Raum T, Kufer P, PENDZIALEK J, Bluemel C, DAHLHOFF C, Hoffmann P, et al. Bispecific antibody constructs binding dll3 and cd3. Google Patents; 2021.
41. Modi S, Saura C, Yamashita T, Park YH, Kim SB, Tamura K, et al. Trastuzumab Deruxtecan in previously treated HER2-Positive breast Cancer. N Engl J Med. 2020;382:610–21.
42. Ogitani Y, Aida T, Hagihara K, Yamaguchi J, Ishii C, Harada N, et al. DS-8201a, A Novel HER2-Targeting ADC with a novel DNA topoisomerase I inhibitor, demonstrates a Promising Antitumor Efficacy with differentiation from T-DM1. Clin Cancer Res. 2016;22:5097–108.
43. Fan P, Xu K. Antibody-drug conjugates in breast cancer: marching from HER2-overexpression into HER2-low. Biochim Biophys Acta Rev Cancer. 2023;1878:188849.
44. Pommier Y, Thomas A. New Life of Topoisomerase I inhibitors as antibody-drug Conjugate warheads. Clin Cancer Res. 2023;29:991–3.

45. Hashimoto Y, Koyama K, Kamai Y, Hirotani K, Ogitani Y, Zembutsu A, et al. A novel HER3-Targeting antibody-drug Conjugate, U3-1402, exhibits potent therapeutic efficacy through the delivery of cytotoxic payload by efficient internalization. Clin Cancer Res. 2019;25:7151–61.
46. Ogitani Y, Hagihara K, Oitate M, Naito H, Agatsuma T. Bystander killing effect of DS-8201a, a novel anti-human epidermal growth factor receptor 2 antibody-drug conjugate, in tumors with human epidermal growth factor receptor 2 heterogeneity. Cancer Sci. 2016;107:1039–46.
47. Johnson ML, Doi T, Piha-Paul SA, Sen S, Shimizu T, Cheng B, et al. 513O A phase I/II multicenter, first-in-human study of DS-7300 (B7-H3 DXd-ADC) in patients (pts) with advanced solid tumors. Ann Oncol. 2021;32:S583–5.
48. Tan X, Fang P, Li K, You M, Cao Y, Xu H, et al. A HER2-targeted antibody-novel DNA topoisomerase I inhibitor conjugate induces durable adaptive antitumor immunity by activating dendritic cells. MAbs. 2023;15:2220466.
49. Nicolò E, Giugliano F, Ascione L, Tarantino P, Corti C, Tolaney SM, et al. Combining antibody-drug conjugates with immunotherapy in solid tumors: current landscape and future perspectives. Cancer Treat Rev. 2022;106:102395.
50. Chung HC, Piha-Paul SA, Lopez-Martin J, Schellens JHM, Kao S, Miller WH Jr., et al. Pembrolizumab after two or more lines of previous therapy in patients with recurrent or metastatic SCLC: results from the KEYNOTE-028 and KEYNOTE-158 studies. J Thorac Oncol. 2020;15:618–27.
51. Petty WJ, Paz-Ares L. Emerging strategies for the treatment of small cell lung Cancer: a review. JAMA Oncol. 2023;9:419–29.

Publisher's Note